3C–6H phase transition in $BaTiO_3$ induced by Fe ions: an electron paramagnetic resonance study

2008 J. Phys.: Condens. Matter 20 505209

(http://iopscience.iop.org/0953-8984/20/50/505209)

J. Phys.: Condens. Matter **20** (2008) 505209 (8pp) doi:10.1088/0953-8984/20/50/505209

3C–6H phase transition in $BaTiO_3$ induced by Fe ions: an electron paramagnetic resonance study

R Böttcher[1,4], H T Langhammer[2], T Müller[3] and H-P Abicht[3]

[1] Fakultät für Physik und Geowissenschaften, Universität Leipzig, Linnéstraße 5, D-04103 Leipzig, Germany
[2] Physikalisches Institut, Martin-Luther-Universität Halle-Wittenberg, Friedemann-Bach-Platz 6, D-06108 Halle, Germany
[3] Chemisches Institut, Martin-Luther-Universität Halle-Wittenberg, Kurt-Mothes-Straße 2, D-06120 Halle, Germany

E-mail: boettch@physik.uni-leipzig.de, hans.langhammer@physik.uni-halle.de, thomas.mueller@chemie.uni-halle.de and hans-peter.abicht@chemie.uni-halle.de

Received 15 July 2008, in final form 1 October 2008
Published 12 November 2008
Online at stacks.iop.org/JPhysCM/20/505209

Abstract
X-ray diffraction (XRD) patterns and electron paramagnetic resonance (EPR) powder spectra (9 and 34 GHz) of $BaTiO_3 + 0.04\ BaO + 0.5x Fe_2O_3$ ($0.0005 \leqslant x \leqslant 0.02$) ceramics were studied to investigate the development of the hexagonal phase (6H modification) of Fe-doped material in dependence upon doping level x and sintering temperature T_s. Three axially symmetric EPR spectra assigned to Fe^{3+} ions substituted at Ti lattice sites corresponding to the different distorted octahedra in tetragonal and hexagonal modification are observed at room temperature. The presence of a hexagonal phase is shown by the XRD pattern and the EPR spectra. The 6H modification begins to occur at a nominal Fe concentration of between $x = 0.005$ and 0.01 and increases with increasing sintering temperature. $BaTiO_3$ ceramics with $x = 0.02$ sintered at $T_s = 1400\,^{\circ}C$ is hexagonal. As discussed in the case of other 3d ions we propose the Jahn–Teller (JT) distortion as the driving force for the cubic–hexagonal transition at high temperatures whereas a sufficiently high concentration of oxygen vacancies is the second condition for this transformation process. In the case of Fe-doped $BaTiO_3$ a minimum concentration of Fe^{4+} in the ceramic grains could trigger the transmutation into the hexagonal phase.

1. Introduction

Barium titanate ($BaTiO_3$) is a material system of fundamental importance for a wide range of technical applications and, because of the variety of phase transitions, a model system of the physical description of the ferroelectricity. Besides the well-known temperature-driven phase transitions (cubic $\xrightarrow{125\,^{\circ}C}$ tetragonal $\xrightarrow{0\,^{\circ}C}$ orthorhombic $\xrightarrow{-90\,^{\circ}C}$ rhombohedral) of the 3C modification this perovskite shows size-driven and defect-induced phase transitions [1–7]. The size-driven transition takes place in nanocrystallites of the 3C polytype if their sizes fall short of a critical size (≈50 nm) depending on the preparation route. In 1960, Glaister *et al* [8] reported that certain amounts of Mn are sufficient to induce the 3C (cubic) to 6H (hexagonal) phase transition and to stabilize the hexagonal phase at room temperature whereas the hexagonal polytype 6H-$BaTiO_3$ (h-$BaTiO_3$) of the undoped material is stable in air at temperatures higher than 1430 °C [9, 10].

h-$BaTiO_3$ crystallizes in the space group $P6_3/mmc$ with the lattice parameters $a = 0.5738$ nm and $c = 1.3965$ nm [11]. The unit cell is described by six BaO_3 layers (i.e. $[Ba(2)O(2)_3Ba(2)O(2)_3Ba(1)O(1)_3]_2$) forming a $(cch)_2$ sequence, where c corresponds to corner-sharing and h to face-sharing layers of the TiO_6 octahedra, respectively (for labelling the atoms see [9]). The Ti(1) atoms occupy the corner-sharing octahedra whereas the Ti(2) atoms are incorporated

[4] Author to whom any correspondence should be addressed.

into the Ti_2O_9 groups of the face-sharing octahedra. In contrast to the cubic crystal structure the octahedra in h-$BaTiO_3$ are trigonally distorted in the c direction. The strength of the trigonal distortion in the corner- and face-sharing octahedra is different. Therefore, there are two different Ti lattice sites in the hexagonal material. Four of the six Ti ions in the hexagonal unit cell are incorporated into the face-sharing octahedra whereas the other two are lying in the exclusively corner-sharing ones.

Two possibilities for the defect-induced phase transition are known to stabilize the hexagonal modification of $BaTiO_3$ at lower temperature than 1430 °C. The first one is firing the 3C modification in a reducing atmosphere (oxygen-deficient $BaTiO_3$) [8, 12]. In a pure hydrogen atmosphere a temperature of 1330 °C is sufficient for the transformation into the hexagonal phase. Doping with some acceptor-type 3d transition elements like Cr, Mn, Fe, Ni or Cu [5–8, 13, 14] as well as with the elements Mg, Al, Ga or In [15] is the second way of stabilizing h-$BaTiO_3$ at room temperature. Grey *et al* [7] reported on the structural analysis of the h-$BaTi_{1-x-y}Fe^{3+}_xFe^{4+}_yO_{3-x/2}$ solid solution with ($0.125 < x < 1$, $y \approx 0$) and ($x \approx 0$, $0.2 < y < 1$) where the Fe^{3+}/Fe^{4+} ratio depends on the reaction temperature and gas atmosphere. For samples with $y \approx 0$ the progressive substitution of Ti^{4+} by Fe^{3+} is accompanied by the formation of O(1) oxygen vacancies in the h-BaO_3 layers that separate pairs of occupied face-shared octahedra. The major structural changes accompanying the progressive removal of the oxygen from the O(1) sites are increasing M(2)–M(2) separations between metal atoms in the binuclear group and increasing Ba(2)–Ba(2) separations. The expansion in the Ba(2)–Ba(2) distance results from the constraints imposed by strong non-bonded Ba(2)–Ba(2) repulsions.

Because of the rather large difference of the effective radii between Ba^{2+} and Ti^{4+}, the incorporation of tri- and higher-valent Fe ions on Ti sites is very probable, which has been supported by EPR investigations [16–22]. Among the investigations by electron paramagnetic resonance, Siegel and Müller [17] investigated the Fe^{3+}_{Ti} ion incorporated into single crystals of the 3C modification and showed that the isolated Fe^{3+} remains at the centre of the oxygen octahedron in all three ferroelectric phases, in contrast to the Ti^{4+} ion which undergoes a cooperative transition. In the tetragonal phase the axial fine structure (FS) parameter D of the Fe^{3+}_{Ti} ion is related to the tetragonal distortion ($c_t/a_t - 1$) of the unit cell with the lattice parameters c_t and a_t, and the substitutional Fe^{3+} detects coherent displacements of intrinsic ions. In the 3C modification Fe is able to bind an oxygen vacancy and to form paramagnetic Fe^{3+}–V_o or Fe^{4+}–V_o associates [21].

In h-$BaTiO_3$ single crystals, the Fe^{3+} spectra have been measured by Ohi *et al* [19]. However, the angular dependence of the resonance fields at room temperature must be explained by an axial spin Hamiltonian and not by an orthorhombic one (see figure 2(c) in [19]). The symmetry axis of the axial fine structure tensor is the hexagonal c axis.

Until now, no systematic investigations of the influence of iron doping on the stabilization of the 6H modification of $BaTiO_3$ ceramics at room temperature with respect to doping level and sintering temperature are known. Hence, an aim of the work is eliminating this lack by means of XRD, EPR and investigation of the microstructure. EPR in different frequency bands was used to characterize the Fe^{3+}_{Ti} defect both in 3C and 6H modifications, depending on doping level and sintering temperature. As already formerly discussed in the case of the dopants Mn [5], Cu [6] and Cr [23] we propose the Jahn–Teller (JT) distortion as the driving force for the cubic–hexagonal phase transition at high temperatures whereas a sufficiently high concentration of oxygen vacancies is the second condition for this transformation process. In the case of Fe-doped $BaTiO_3$ a minimum concentration of Fe^{4+} (electron configuration d^4, strong JT effect) in the ceramic grains could trigger the transmutation into the hexagonal phase. Since the cubic–hexagonal phase transition takes place at temperatures >1200 °C, depending on oxygen partial pressure, the kind of dopant and doping level, it is very difficult, or nowadays probably impossible, to perform *in situ* measurements which could give information about the details of the JT distortion which initiates the microscopic steps of the phase transformation (reciprocal gliding of (111) lattice planes [5]) according to our hypothesis.

2. Experimental procedure

Ceramic powders with the nominal composition $BaTiO_3 + 0.04\ BaO + 0.5x Fe_2O_3$ ($0.0005 \leqslant x \leqslant 0.02$) were prepared by the conventional mixed-oxide powder technique. After the mixing (agate balls, water) and calcining (1100 °C, 2 h) of $BaCO_3$ (Solvay, VL600, <0.1 mol% Sr) and TiO_2 (Merck, no. 808), Fe_2O_3 (Merck, p.a.) was added to the $BaTiO_3$ powder. Then it was fine-milled (agate balls, 2-propanol) and densified into discs with a diameter of 6 mm and a height of nearly 3 mm. The samples were sintered in air at temperatures of 1300, 1350 and 1400 °C for 1 h (heating rate 10 K min^{-1}).

The microstructure of the sintered specimens was examined by optical microscopy. The overall phase composition was determined quantitatively by analysing the XRD intensity ratios (peak heights) $(111)_{tetragonal}/(103)_{hexagonal}$ and $(200)_{tetragonal}/(103)_{hexagonal}$ calibrated by well-defined mixtures of pure tetragonal and hexagonal barium titanate powders (STADI MP diffractometer, STOE, Germany). EPR measurements of finely pulverized samples were carried out in the X-band (9 GHz) with a Varian E 112 spectrometer and in the Q-band (34 GHz) with a Bruker EMX device. More details of the measuring procedure are described in [24]. For evaluation of the powder EPR spectra and the determination of the spin Hamiltonian parameters the MATLAB[5] toolbox for electron paramagnetic resonance 'Easy Spin 2.0.3' was used [25]. By simultaneously simulating the X- and Q-band powder spectra by variation of the parameters of the standard spin Hamiltonian, equation (1), for the high-spin system Fe^{3+} ($S = 5/2$), a satisfactory accuracy in the determination of the spectral parameters was achieved. The spin Hamiltonian used with isotropic Zeeman term is

$$\hat{H} = \beta g \vec{B} \hat{\vec{S}} + \frac{D}{3} \hat{O}_2^0 + \hat{H}_{cub} \qquad (1)$$

[5] MATLAB is a registered trademark of MathWorks, Inc., Natick, MA, USA.

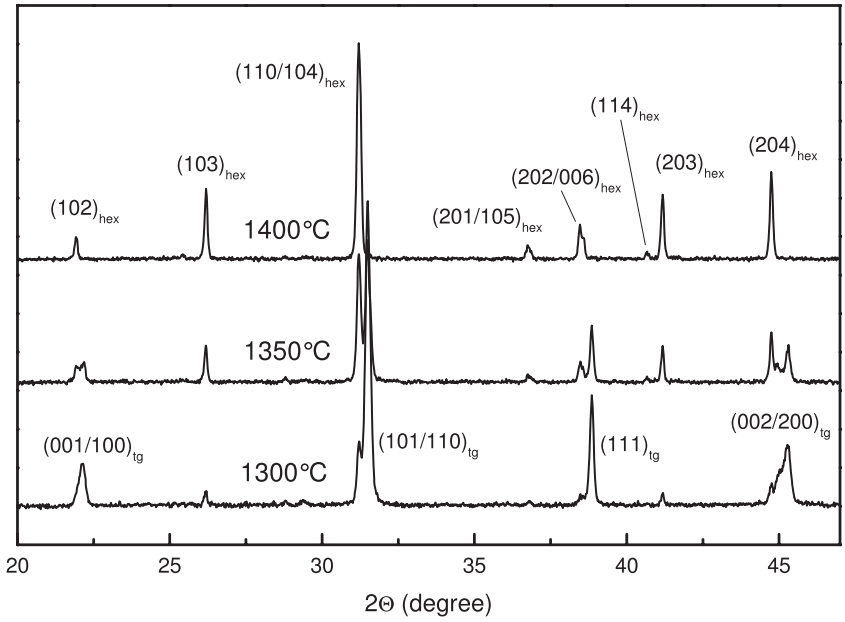

Figure 1. XRD diagrams of the sample with $x = 0.02$ (2 mol% Fe) sintered at different temperatures T_s ($T_s = 1300$, 1350 and 1400 °C).

with the fine structure Hamiltonian $\hat{H}_{\rm cub}$ for cubic fields. This fourth-degree cubic operator may be written as $\frac{a}{120}(\hat{O}_4^0 + 5\hat{O}_4^4)$ or $-\frac{a}{180}(\hat{O}_4^0 + 20\hat{O}_4^3)$, where the first form refers to a fourfold z axis (3C modification) and the second to a threefold z axis (6H modification). The extended Stevens operators $\hat{O}_k^q$ are given in [26]. The parameters used have the meaning: g the electronic g factor, β the Bohr magneton, D the axial and a the cubic fine structure (FS) parameter, respectively. The axial fourth-order parameter F is smaller than 5×10^{-4} cm^{-1}. Therefore, it was not included in the simulation of the spectra. The assumption that all Fe ions in the 3C or 6H $BaTiO_3$ powder sample can be modelled by the same set of spin Hamiltonian parameters is hardly ever applicable because the local symmetry of the paramagnetic ion is distorted by strain effects. For the high-spin Fe^{3+} ion ($S = 5/2$) we used only a distribution of the fine structure parameter D. Assuming random fluctuations in the local lattice parameters in the vicinity of the paramagnetic impurity the distribution of this FS parameter can be approximated by a Gaussian with the full width at half-height (FWHH) ΔD.

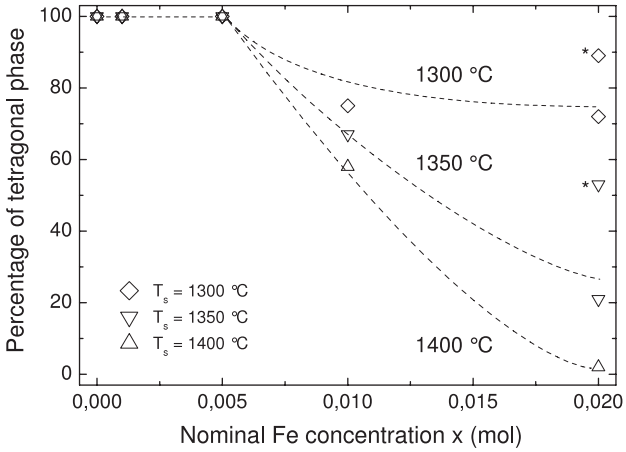

Figure 2. Room-temperature percentage of tetragonal phase of Fe-doped $BaTiO_3$ sintered at 1300 °C, 1350 °C and 1400 °C, respectively, as a function of the nominal Fe concentration. Data points marked by an asterisk refer to samples to which dopant was already added before the calcining process. The accuracy of the percentage data is not better than 10%.

3. Results

3.1. XRD and microstructure

Figure 1 shows the XRD pattern of the samples with 2 mol% Fe ($x = 0.02$) as a function of the sintering temperature. Each of these powder patterns is a superposition of two others which are assigned to the 3C and 6H modification of barium titanate. The hexagonal portion increases with increasing sintering temperature T_s, and at $T_s = 1400$ °C only negligible traces of the tetragonal phase are detected. The dependence of the portion of the tetragonal phase on the nominal Fe content is shown in figure 2. The 6H modification begins to occur at a nominal concentration of between 0.5 and 1.0 mol% Fe. The corresponding microstructure data are shown in figure 3. Interestingly, the development of the microstructure for the Fe-doped, Ba-rich samples is rather unusual. Whereas the undoped samples exhibit normal grain growth behaviour with globular grains of about 5 μm in size ($T_s = 1400$ °C), the sample with $x = 0.001$ shows exaggerated grain growth with a mean grain size of about 50 μm even at the lowest sintering temperature of 1300 °C. The grains look cube-like with aspect ratios of nearly one. With increasing Fe content this grain growth gradually diminishes and the mean grain size of the samples with $x = 0.02$ is similar to that of the undoped samples. Obviously, Fe_2O_3 forms a eutectic in the system Fe_2O_3–BaO–TiO_2, which melts below 1300 °C, promoting the

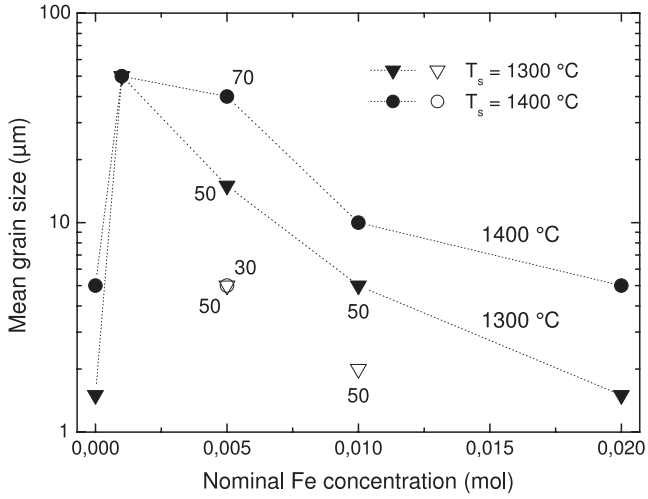

Figure 3. Average grain sizes of $BaTiO_3$ ceramics as a function of the nominal Fe concentration. Hollow/solid symbols mean different fractions of a bimodal microstructure. Numbers at data symbols denote the portions of these grain fractions, roughly estimated manually from the areas in a two-dimensional sample cut.

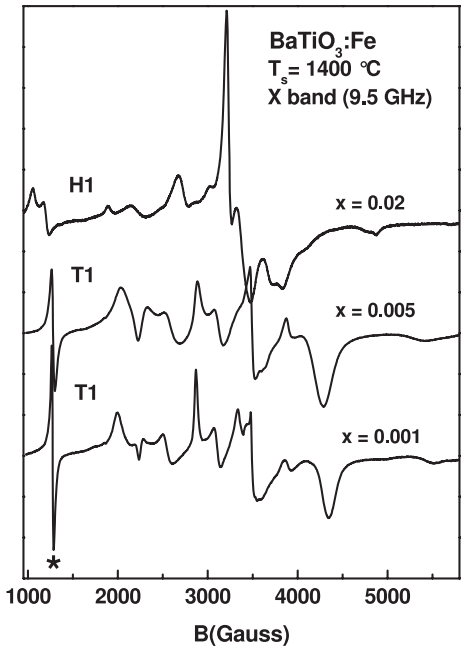

Figure 4. Room-temperature EPR spectra of $BaTiO_3$ samples sintered at 1400 °C in dependence upon the Fe concentration x ($x = 0.001$, 0.005 and 0.02), measured in the X-band (9.5 GHz). In the T1 spectrum the peak of the forbidden transition $\Delta M_S = \pm 2$ ($M_S = 1/2 \leftrightarrow M_S = -3/2$) is designated by an asterisk.

exaggerated grain growth already with rather small amounts of Fe_2O_3. At higher amounts of Fe_2O_3 the gradually suppressed grain growth is possibly caused by the relatively large amounts of liquid phase which hinder the liquid-phase-assisted grain growth [27]. A steep liquidus line between $BaTiO_3$ and the eutectic composition could explain these high amounts of liquid phase even at a rather low doping concentration. Because of the hindered ($x = 0.01$) or nearly suppressed ($x = 0.02$) liquid-phase-assisted exaggerated grain growth, large plate-like grains which are typical for h-$BaTiO_3$ [5, 28] occur only here and there in the samples with $x = 0.01$ whereas the samples with $x = 0.02$ exhibit small plate-like grains (mean size 5 μm, aspect ratio about 3:1) at $T_s \geqslant 1350$ °C.

3.2. EPR

Figure 4 reveals the EPR powder spectra of the samples with $x = 0.001$, 0.005 and 0.02 sintered at 1400 °C. In the case of $x = 0.001$ the tetragonal spectrum (called T1) is identical with that of Fe-doped 3C-$BaTiO_3$ reported by Schwartz and Wechsler [22] who labelled the peaks of the powder spectrum with the corresponding electronic spin quantum numbers and the canonical orientations of the crystallites with respect to the external magnetic field. This X-band spectrum consists of allowed ($\Delta M_S = \pm 1$) and forbidden ($\Delta M_S = \pm 2$, ...) FS peaks and can be explained by the spin Hamiltonian for the $S = 5/2$ high-spin system, equation (1), with the axial FS parameter D ($D \approx h\nu$, ν the X-band microwave frequency) and the cubic FS term $\frac{a}{120}(\hat{O}_4^0 + 5\hat{O}_4^4)$ (cubic FS constant a). The spin Hamiltonian parameters (given in table 1) were estimated by simultaneous simulation of the X-and Q-band powder spectra and agree with the single-crystal [17] and powder [22] measurement results. Therefore, the assignment of the spectrum to Fe^{3+} ions in crystallites of the 3C modification of $BaTiO_3$ is unambiguous. The peaks are broadened by random stress effects characterized by static fluctuations of the axial FS parameter D which are accounted for by a Gaussian with the full width at half-height (FWHH) ΔD. Increasing the Fe concentration in the samples, an additional line with $g \approx 2.00$ (called the T2 spectrum) appears and the peaks of the T1 powder spectrum are broadened by dipole–dipole interaction and random stress effects (see the spectrum with $x = 0.005$ in figures 4 and 5). Due to the higher Fe concentration the $BaTiO_3$ lattice is locally distorted close to the impurity ion and the unit cell parameters are changed. The axial FS parameter D decreases and the FWHH of the axial FS distribution increases. On going to an Fe concentration of $x = 0.02$ the powder spectrum drastically changes its shape and a new spectrum (labelled by H1) with poorly resolved FS peaks in the X-band appears. Because of the higher microwave frequency, the Q-band spectrum (figure 5) has fewer peaks and consequently a higher resolution which permits a assignment of the peaks to allowed FS transitions with the selection rules $\Delta M_s = \pm 1$ and special orientations of the crystallites with respect to the external magnetic field (figure 6). The number of allowed FS peaks affords the determination of the electronic spin quantum number S and thus the charge state of the Fe impurity. As a result of $S = 5/2$ the charge state of this Fe defect must be 3+. The spin Hamiltonian with the cubic FS term $-\frac{a}{180}(\hat{O}_4^0 + 20\hat{O}_4^3)$, equation (1), was used for the spectrum simulation and the determination of its spectral parameters (figure 7). The results are given in table 1. Our FS parameter D agrees with the absolute value of Ohi *et al* [19] who deduced this parameter from the angular dependences of the EPR spectra of hexagonal $BaTiO_3$ single crystals. In contrast to the results in [19] the powder spectra confirmed unambiguously the local axial symmetry of the lattice site of the Fe^{3+} ion.

Table 1. Room-temperature spin Hamiltonian parameters and the hexagonal portion of the $BaTiO_3$ samples doped with 100× mol% Fe in comparison with literature values.

Sample x/T_s (°C)	g factor	Axial FS parameter D (10^{-4} cm^{-1})	Cubic FS parameter a (10^{-4} cm^{-1})	FWHH ΔD (10^{-4} cm^{-1})	Hexagonal portion[a] (%)	Remarks
0.0005/1300–1400[b]	2.0045(5)	930(30)	110(10)	40(10)	0	T1
0.0010/1300–1400[b]	2.0045(5)	920(30)	110(10)	150(20)	0	T1
0.0050/1300–1400[b]	2.0045(5)	850(50)	110(10)	200(30)	0	T1(80%)[d]
	2.0045(10)	450(80)	[c]	550(100)		T2(20%)[d]
0.0200/1300	2.0045(10)	450(80)	[c]	550(100)	11	T2
0.0200/1350	2.0055(5)	590(30)	140(5)	40(10)	47	H1(40%)[d]
	2.0045(10)	450(80)	[c]	550(100)		T2(60%)[d]
0.0200/1400	2.0055(5)	590(30)	140(5)	40(10)	98	H1(100 %)[d]
0.0005/crystal	2.0036	929	91	[e]	0	T1 [17, 18]
0.0100/powder	2.00	[e]	[e]	[e]	0	T2 [29]
0.0005/crystal	2.00	−590	59	[e]	100	H1 [19]

[a] Determined by XRD.
[b] Spin Hamiltonian parameters are independent of the sintering temperature.
[c] Not quantifiable.
[d] Estimated spectral intensity.
[e] Not determined.

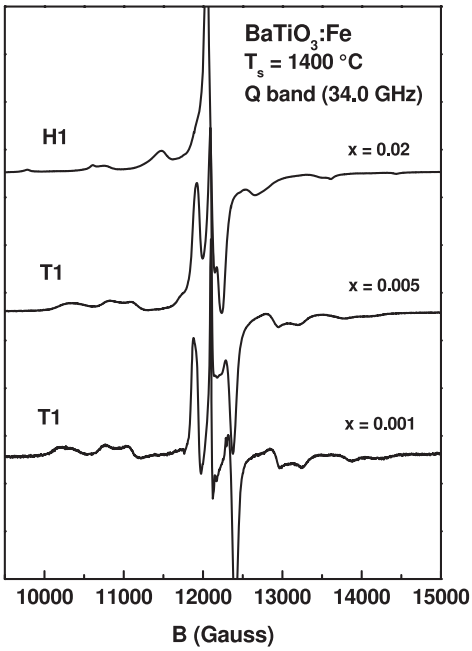

Figure 5. Room-temperature EPR spectra of $BaTiO_3$ samples sintered at 1400 °C in dependence upon the Fe concentration x ($x = 0.001$, 0.005 and 0.02) measured in the Q-band (34.0 GHz).

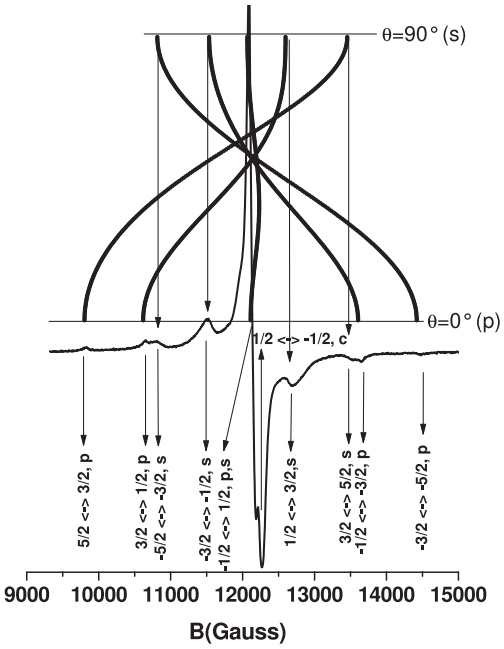

Figure 6. H1 spectrum (Q-band, room temperature) of the 2 mol% ($x = 0.02$) Fe-doped $BaTiO_3$ sample sintered at 1400 °C (lower part). The peaks were assigned to the allowed transitions $\Delta M_S = \pm 1$ by comparing the theoretical rotation pattern (upper part). The resonance fields were calculated with the experimentally determined spin Hamiltonian parameters of the H1 centre, given in table 1. The angle θ is the angle between the external magnetic field B and the hexagonal c axis (symmetry axis of the spin-Hamiltonian operator), p (parallel), s (perpendicular) and c conform to the rotation angles $\theta = 0°$, $\theta = 90°$ and $\theta \approx 42°$, respectively.

Figure 8 represents the room-temperature spectra of 2 mol% Fe ($x = 0.02$)-doped $BaTiO_3$ prepared under different sintering temperatures T_s ($T_s = 1300$, 1350 and 1400 °C). The 1300 °C sample has a very simple EPR spectrum consisting of a nearly symmetric line with $g \approx 2.00$ which corresponds to the T2 spectrum of the sample with $x = 0.005$. Additional peaks with very small intensities were observed in the low-field range of the X-band spectrum. At first, this T2 spectrum was detected by Hagemann [29] in Fe-doped (1 mol%) $BaTiO_3$ ceramics with 3C modification. Because the information content of this spectrum is poor its temperature dependence was studied. Close to the tetragonal–cubic phase transition temperature $T_c = 125$ °C strong changes in the width and intensity of the $g \approx 2$ line were detected because the local symmetry of the Fe ion is now cubic (axial FS parameter $D = 0$). Using the spin Hamiltonian with the cubic term

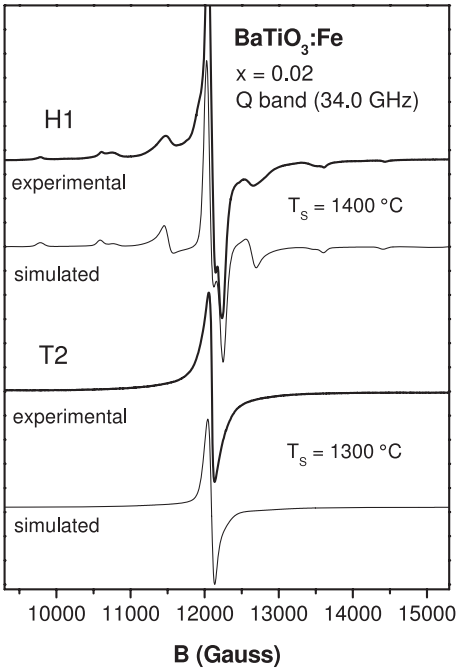

Figure 7. Experimental and simulated Q-band spectra of the 2 mol% Fe-doped $BaTiO_3$ for $T_S = 1300$ and 1400 °C. For the simulation the spin Hamiltonian (1) and the parameters given in table 1 were used.

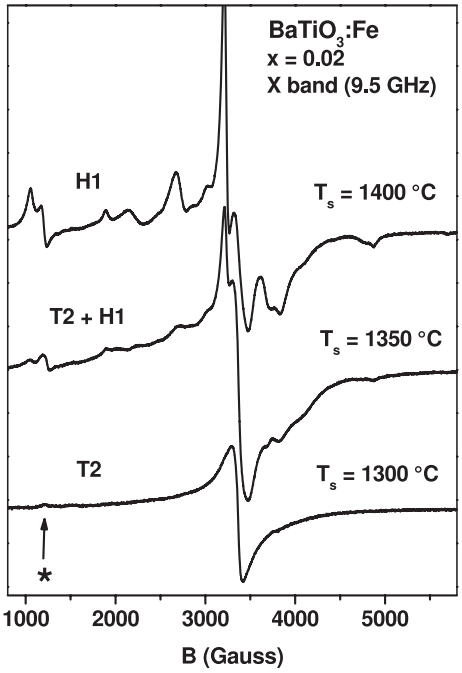

Figure 8. Room-temperature EPR spectra of the 2 mol% ($x = 0.02$) Fe-doped $BaTiO_3$ samples in dependence upon the sinter temperature T_s ($T_s = 1300$, 1350, 1400 °C), measured in the X-band (9.5 GHz). The peak of the forbidden transition $\Delta M_S = \pm 2$ ($M_S = 1/2 \leftrightarrow M_S = -3/2$) is designated by an asterisk.

$\frac{a}{120}(\hat{O}_4^0 + 5\hat{O}_4^4)$, equation (1), and $S = 5/2$, systematic spectral simulations show that the T2 spectrum can be simulated with a reduced axial FS parameter D, increased individual linewidth and the FWHH of the axial FS parameter distribution (figure 7). The best-fit parameters are given in table 1. The structure of the EPR powder pattern of the sample with $x = 0.02$ is dependent on the temperature of the sintering process. On increasing it by 50 K changes in the EPR powder pattern are observed. The spectrum of the 1350 °C sample is a superposition of the T2 and H1 spectra with nearly equal intensities whereas in the 1400 °C sample only the H1 spectrum is measured (figure 8).

4. Discussion

The doping ion iron can substitute Ti in the 3C and 6H modification of barium titanate, exhibiting oxidation states of 2+ (free-ion electron configuration d^6, ground state ^5D with $S = 2$), 3+ (d^5, ^6S with $S = 5/2$), 4+ (d^4, ^5D with $S = 2$) and 5+ (d^3, ^4F with $S = 3/2$). Because of the weak spin–lattice interaction of the non-degenerated orbital ground states in electrical crystalline fields of octahedral symmetry only the oxidation states of the Fe impurities 3+ ($S = 5/2$) and 5+ ($S = 3/2$) are detectable with EPR spectroscopy. In all our experiments we have not observed any EPR spectrum which can be described by an electron spin $S = 3/2$. Consequently, Fe^{5+} ions do not exist in the samples.

Because the Fermi level is pinned by the Fe^{3+}/Fe^{4+} ionization level in Fe-doped $BaTiO_3$ samples the iron has the valence states of 3+ and 4+ (room temperature), with a distinctly higher Fe^{3+} portion [28]. Thus, Fe^{4+} probably plays the role of the JT-active ion which causes the cubic–hexagonal phase transformation at temperatures below 1430 °C (transition temperature of undoped $BaTiO_3$). Obviously, in the lower-doped samples ($x = 0.001$ and 0.005) the concentration of Fe^{4+} is too low to induce the transmutation from the 3C to the 6H modification even at the highest sintering temperature of 1400 °C, since all samples investigated are completely tetragonal. The negative charge of the Fe_{Ti}^{3+} ions (relative to the Ti^{4+} lattice site) is compensated by the formation of positive oxygen vacancies which are not associated with Fe^{3+} ions [21]. Iron impurities and vacancies produce local deformations in the crystallites and induce changes in the lattice parameters which influence the spectral parameters of the axial Fe_{Ti}^{3+} spectrum. The fall of the axial FS parameter D with increasing Fe concentration is the direct consequence of the decrease of the tetragonal distortion parameter $(c_t/a_t - 1)$ of the unit cell. Already, Hagemann showed that the parameter $(c_t/a_t - 1)$ is a linear function of the Fe concentration in the range up to 1.5 mol% and is constant at concentrations $\geqslant$2 mol% [29].

Due to the high concentration of iron and the oxygen vacancies in the sample with $x = 0.02$, the parameter $(c_t/a_t - 1)$ is more reduced, the strain is grown on in the crystallites and the mean distance of neighbouring Fe^{3+} ions is reduced. The reduction of $(c_t/a_t - 1)$ brings about a decrease of the FS parameter D whereas the strain effect (increasing FWHH of the D parameter distribution) and dipole–dipole interaction cause strong linewidth broadening in the Fe^{3+} spectrum. Hence, the FS peaks, whose resonance fields are linearly dependent on the axial FS parameter D, are broadened and are no longer detectable in the powder pattern (figure 8, $T_s = 1300$ °C). The central transition $M_S = +1/2 \leftrightarrow M_S = -1/2$ is observed

as a nearly symmetric line (spectrum T2), whose width is a measure of the dispersion (FWHH) of the axial fine structure parameter due to lattice deformation. The low-field peak in the X-band spectrum, designated by an asterisk in figure 8, belongs to this axial spectrum and is assigned to the forbidden transition $\Delta M_S = \pm 2$ with the spin quantum numbers $M_S = 1/2$ and $M_S = -3/2$. Its position in the spectrum is nearly independent of the D parameter. The T2 spectrum is assigned to Fe^{3+} ions substituted for Ti^{4+} in distorted octahedral surroundings of the 3C modification with changed lattice parameters. In spite of the high doping level this material is still ferroelectric and the temperature-driven phase transition can be detected by means of EPR spectroscopy by investigating the temperature dependence of the T2 spectrum. At the tetragonal–cubic phase transition temperature, the tetragonal FS parameter drops to zero and the intensity of the line with $g \approx 2.00$ grows on, as observed in the experiment. The dopant Fe is homogeneously incorporated in the $BaTiO_3$ grains up to the concentration of 1.5 mol% [29, 30]. Therefore, it is assumed that in samples with $x = 0.02$ the majority of the Fe^{3+} ions is substituted at the Ti^{4+} sites in the grains. Only a smaller fraction is present as pairs and aggregations of Fe^{3+} ions in the crystallites and/or grain boundaries, which cannot be detected by EPR.

Because of the high iron concentration and its non-uniform distribution within the samples with $x = 0.02$, some grains exhibit a local Fe^{4+} concentration which exceeds the critical value, triggering the transmutation to the hexagonal phase already for the sample sintered at 1350 °C. In these hexagonal crystallites the surrounding of the paramagnetic Fe^{3+} ion is changed and the H1 spectrum appears. Because the Fe^{4+} concentration has not reached the critical value in all grains there are also grains with tetragonal symmetry. Thus, the corresponding EPR powder pattern of the sample ($x = 0.02$, $T_S = 1350$ °C) is a superposition of the tetragonal (T2) and hexagonal (H1) spectra. Obviously, the H1 spectrum of the sample sintered at 1300 °C, which is already 11% hexagonal (XRD), is covered up by the strong T2 spectrum.

Increasing the sintering temperature the concentration of Schottky-type oxygen vacancies increases which reduces Ti^{4+} to Ti^{3+} (see equation (2))[6] and consequently the concentration of Ti^{3+} increases:

$$2\mathrm{Ti}_{\mathrm{Ti}}^{x(4+)} + \mathrm{O}_{\mathrm{O}}^{x} \rightleftharpoons \mathrm{V}_{\mathrm{O}}^{\cdot\cdot} + 2\mathrm{Ti}_{\mathrm{Ti}}^{\prime(3+)} + \tfrac{1}{2}\mathrm{O}_2\uparrow. \qquad (2)$$

Since Ti^{3+} is also a JT-active ion (electron configuration d^1, weak JT effect), which triggers the phase transformation cubic–hexagonal in undoped $BaTiO_3$ [5], the total concentration of JT-active ions (Fe^{4+} and Ti^{3+}) increases and the portion of hexagonal crystallites, and consequently the intensity of the H1 spectrum, further increases (figure 8). In the 2 mol% Fe-doped sample sintered at 1400 °C the hexagonal portion is nearly 100% and the H1 spectrum is dominant in the EPR powder pattern and hence the T2 spectrum is not longer conspicuous. Compared to the other acceptor dopants which we investigated systematically up to now, iron and manganese [5] have a similar effectiveness in the lowering of the formation temperature of h-$BaTiO_3$, whereas distinctly lower concentrations of copper [6] and chromium [23] are necessary to initiate the transmutation into the 6H stacking of barium titanate.

The question of the incorporation site of the EPR-active Fe^{3+} ion remains, since h-$BaTiO_3$ has two crystallographically different Ti lattice sites, Ti(1) and Ti(2). If the Fe^{3+} ions would be incorporated on both Ti sites, two different powder spectra with unequal spin Hamiltonian parameters are expected. However, only one type, the H1 spectrum, is observed in the 6H modification. As in the case of the Mn^{4+} ion [31] Fe^{3+} ions are incorporated only on the Ti(1) lattice sites in exclusively corner-sharing octahedra in which the six Ti(1)–O(2) distances are equal. Due to the hexagonal structure the local symmetry of the Ti(1) site is reduced to the trigonal one by the presence of the next-nearest neighbours. In comparison with the Ti(2) site, the electrical trigonal field, which is responsible for the fine structure splitting, is weaker at the Ti(1) site.

5. Conclusions

Fe-doped $BaTiO_3$ ceramics (Ba:Ti = 1.04) sintered at 1400 °C in air change their room-temperature crystallographic structure gradually from tetragonal to hexagonal, beginning with Fe concentrations between 0.5 and 1.0 mol%. In the tetragonal 3C modification the shape of the EPR powder spectrum is dependent on the Fe concentration. In low-doped material the T1 spectrum with many fine structure peaks is detected whereas the sample with $x = 0.02$ ($T_s = 1300$ °C) has only the single-line spectrum T2 arising from the T1 by the decrease of the D parameter and increase of broadening effects due to D-strain and dipole–dipole interaction. EPR measurements revealed that in both modifications Fe^{3+} is incorporated at Ti sites. In the hexagonal phase Fe^{3+} occupies only Ti(1) sites (exclusively corner-sharing oxygen octahedra). We suggest that the high temperature cubic–hexagonal phase transition is driven by a Jahn–Teller distortion caused by EPR-silent Fe^{4+}, analogously to the cases of Mn-, Cu- and Cr-doped $BaTiO_3$ with the JT-active ions Mn^{3+}, Cu^{2+} and Cr^{4+}, respectively. The liquid-phase-assisted exaggerated grain growth even at iron concentrations of 0.1 mol% is caused by a low-melting eutectic in the system Fe_2O_3–BaO–TiO_2 with a steep liquidus line between $BaTiO_3$ and the eutectic composition.

Acknowledgments

The authors thank Mrs U Heinich and Dipl.-Ing. J Hoentsch for the measurements of the EPR spectra.

References

[1] Anliker M, Brügger H R and Känzig W 1954 *Helv. Phys. Acta* **27** 99
[2] Frey M H and Payne D A 1996 *Phys. Rev.* B **54** 3158
[3] Uchino K, Sadanaga E and Hirose T 1998 *J. Am. Ceram. Soc.* **72** 1555
[4] Böttcher R, Klimm C, Michel D, Semmelhack H-C, Völkel G, Gläsel H-J and Hartmann E 2000 *Phys. Rev.* B **62** 2085

[6] Here the Kröger–Vink notation of point defects is used.

[5] Langhammer H T, Müller T, Felgner K-H and Abicht H-P 2000 *J. Am. Ceram. Soc.* **83** 605
[6] Langhammer H T, Müller T, Böttcher R and Abicht H-P 2003 *Solid State Sci.* **5** 965
[7] Grey J E, Li Ch, Cranswick L M D, Roth R S and Vanderah T A 1998 *J. Solid State Chem.* **135** 312
[8] Glaister R M and Kay H F 1960 *Proc. Phys. Soc.* **76** 763
[9] Burbank R D and Evans H T Jr 1948 *Acta Crystallogr.* **1** 330
[10] Kirby K W and Wechsler B A 1991 *J. Am. Ceram. Soc.* **74** 1841
[11] Akimoto J, Gotoh Y and Oosawa Y 1994 *Acta Crystallogr.* C **50** 160
[12] Sinclair D C, Skakke J M S, Morrison F D, Smith R I and Beales T P 1999 *J. Mater. Chem.* **9** 1327
[13] Ren F, Ishida S and Mineta S 1994 *J. Ceram. Soc. Japan* **102** 3026
[14] Dickson J G, Katz L and Ward R 1961 *J. Am. Chem. Soc.* **83** 3026
[15] Keith G M, Rampling M J, Sarma K, McAlford N and Sinclair D C 2004 *J. Eur. Ceram. Soc.* **24** 1721
[16] Sakudo T 1963 *J. Phys. Soc. Japan* **18** 1626
[17] Siegel E and Müller K A 1979 *Phys. Rev.* B **20** 3587
[18] Müller K A and Berlinger W 1986 *Phys. Rev.* B **34** 6130
[19] Ohi K, Arai H, Ishige T and Shimokoshi M 1989 *J. Phys. Soc. Japan* **58** 3781
[20] Shimokoshi M and Ohi K 1990 *J. Phys. Soc. Japan* **59** 3629
[21] Possenriede R, Jakobs P and Schirmer O F 1992 *J. Phys.: Condens. Matter* **4** 4719
[22] Schwartz R N and Wechsler B A 1993 *Phys. Rev.* B **48** 7057
Schwartz R N and Wechsler B A 1994 *Phys. Rev.* B **50** 659 (erratum)
[23] Langhammer H T, Müller T, Böttcher R and Abicht H-P 2008 *J. Phys.: Condens. Matter* **20** 085206
[24] Böttcher R, Erdem E, Langhammer H T, Müller T and Abicht H-P 2005 *J. Phys.: Condens. Matter* **17** 2763
[25] Stoll St 2003 Spectral simulations in solid-state EPR *PhD Thesis* ETH Zurich
[26] Abragam A and Bleaney B 1970 *Electron Paramagnetic Resonance of Transition Ions* (Oxford: Clarendon)
[27] Hennings D F K, Janssen R and Reynen P J L 1987 *J. Am. Ceram. Soc.* **70** 23
[28] Kolar D, Kunaver U and Rečnik A 1998 *Phys. Status Solidi* a **166** 219
[29] Hagemann H-J 1980 *Dissertation* Rheinisch–Westfälische Technische Hochschule, Aachen
[30] Hagemann H-J and Ihrig H 1979 *Phys. Rev.* B **20** 3871
[31] Böttcher R, Langhammer H T, Müller T and Abicht H-P 2005 *J. Phys.: Condens. Matter* **17** 4925